

# Precise determination of deep trap signatures and their relative and absolute concentrations in semi-insulating GaAs

M. Pavlović<sup>a)</sup> and U. V. Desnica

*Rudjer Bošković Institute, Bijenička 54, 10000 Zagreb, Croatia*

(Received 24 November 1997; accepted for publication 11 May 1998)

The new analytical method, simultaneous multiple peak analysis (SIMPA) which comprises simultaneous fitting of whole measured thermally stimulated current (TSC) spectra is presented. The procedure clearly resolves contributions from various overlapping TSC peaks, which results in precise determination of trap parameters (signature) for each trap. In combination with photocurrent temperature dependent measurements,  $I_{PC}(T)$ , which reflects free carrier lifetime temperature dependence, the estimates of relative and absolute trap concentrations were made as well. The advantage of the SIMPA method in comparison with the single peak approach was demonstrated and analyzed. The SIMPA method was applied to different semi-insulating (SI) GaAs samples, particularly to samples having very high and others having very low deep trap concentrations; and for both extremes excellent fits were achieved. The method also seems very promising for characterization of deep levels and other similar SI materials, like SI InP or SI CdTe. © 1998 American Institute of Physics. [S0021-8979(98)03516-6]

## I. INTRODUCTION

Undoped, semi-insulating (SI) GaAs is an important material often used as a substrate for integrated circuit (IC) and field effect transistor (FET) technologies. The performance of those devices is greatly influenced by the quality of the substrate, which depends on the concentration of native defects and chemical impurities having deep energy levels in band gap. Hence, it is very important to monitor, understand, and control defects with deep levels related to the SI properties in order to produce high quality substrates.

The main deep donor level, the well known—EL2, situated in the middle of the forbidden energy gap, enables high resistivity of the undoped GaAs crystals by compensation of residual shallow acceptors. Beside the omnipresent EL2 level there are some other defects with deep levels in the SI GaAs energy gap for which it was recently found that they also play an important role in low-temperature transient phenomena like photosensitivity,<sup>1-6</sup> Hall mobility,<sup>7</sup> and electron paramagnetic resonance (EPR) signals.<sup>8,9</sup> Furthermore, they also affect temperature dependence of photoconductivity<sup>2,10,11</sup> and persistent photocurrents.<sup>2,11</sup> Several of these levels show metastability-like behavior similar to that of the EL2 level<sup>3,12</sup> indicating a possible microscopical connection between EL2 and some of those defects. It has also been shown that most of these defects are electron traps.<sup>13-15</sup>

The objective of characterization of deep traps is the determination of their main parameters, particularly activation energy ( $E_a$ ) and capture cross section ( $\sigma_n$ ) (“trap signature”), as well as determination of trap concentration ( $N_T$ ). That has been the object of the investigation of many different research groups, and these results were recently analyzed and systematized.<sup>16</sup> As visible from this review,

most reports give only limited and insufficient trap parameters, primarily  $T_m$  (temperature at which particular peak has maximum) and  $E_a$ . The  $\sigma_n$  as well as trap concentrations were rarely evaluated and in most cases only for few dominant traps.<sup>13,14,17,18</sup> Great discrepancies in reported main trap parameters are obvious; for example, up to four orders of magnitude for  $\sigma_n$ .<sup>16</sup>

The reason for such large differences in reported data for the same peaks, as well as the incompleteness of data for most of the deep traps in SI-GaAs, lays in the imperfection of analytical methods applied, different approximations<sup>16</sup> assumed, and particularly in the fact that all these methods are based on a single peak analysis. Since in almost all present SI GaAs materials a number of deep levels are present, the interference of various peaks is practically inevitable, particularly in cases when different traps have very similar  $T_m$ .

For determination and characterization of deep levels in SI materials thermally stimulated current (TSC) spectroscopy is a well-known and often used method,<sup>1,2,10,12-16</sup> especially because capacitance methods [like deep level transient spectroscopy (DLTS)] cannot be applied. The simplicity is an additional advantage of TSC, since it gives qualitative information on various deep levels in a single temperature run. The trap's signatures deduced from the single TSC peak analysis are reliable if (a) only one trap is active in a reasonable temperature range and (b) kinetics order is known so that appropriate approximations could be used. Usually, neither (a) nor (b) are satisfied simultaneously and values deduced by different researchers differ significantly. When the TSC spectrum is formed from the contributions of closely spaced levels, in single peak analysis it is necessary to perform a “thermal cleaning procedure” or some other procedure which facilitates the isolation of the peaks which appear in the complex spectrum. Errors obtained in such single peak treatments are just summed up and propagated to further characterization, where  $E_a$  has to be determined from

<sup>a)</sup>Electronic mail: pavlovic@rudjer.irb.hr

Arrhenius plots or with some approximate formulas.<sup>16,17</sup>

The interpretation of TSC spectra is complicated since measured peak positions are quite dependent on various parameters. In Ref. 19 the dependence of a TSC peak on the heating rate, capture cross section, kinetics order, and initial trap occupancy was demonstrated. The peak position can be significantly shifted (in some cases several tens of Kelvin) by each of the above-mentioned parameters, so that an evaluation of activation energies exclusively from the peak temperature  $T_m$  results in large uncertainties. Furthermore, the existence of different traps which release their charge carriers simultaneously may lead to an additional temperature shift of apparent peak maximum. Once the  $E_a$  is determined, another important parameter,  $\sigma$  can be estimated.<sup>16</sup> Since  $\sigma$  varies exponentially with  $E_a$ , even small errors in  $E_a$  greatly magnify errors in  $\sigma$ 's. There are some modified TSC measurement techniques like "fractional thermally stimulated currents" (FTSC)<sup>19</sup> which improved the reliability of interpretation of TSC data. However, the inability to resolve overlapping peaks, inaccessible weak levels, and levels related to peaks under 100 K, the stabilization of thermal equilibrium at certain temperatures and multiply prolonged time of measurements in manifold heating-cooling (initial rise-initial fall) cycling<sup>19</sup> still remain as problems.

Besides above methods, photoinduced transient spectroscopy (PITS),<sup>16,20-23</sup> which is based on the analysis of thermal behavior of photocurrent transients induced by light pulses is also widely used in detection and characterization of deep traps in Si-GaAs substrates.<sup>16,20,22-24</sup> However, this method also has severe problems due to limited rate windows, assumptions regarding the exponential nature of photocurrent transients, appearance of negative peaks, etc., which makes it less suited for detailed studies, although it is convenient as a general purpose survey technique.

In this paper we are presenting a new analytical method which enables simultaneous fitting of the whole measured conventional TSC spectra. Simultaneous multiple peak analysis (SIMPA) method overcomes most problems of the above-mentioned single peak methods. It enables simultaneous determination of main peak parameters of all traps present in the material. In the fitting procedure signatures of all traps are determined simultaneously, so that the sum of the errors for all traps is minimized. Furthermore, SIMPA clearly indicates where TSC peaks are "missing" and shows when peaks are composite. The method also enables characterization of small TSC peaks even if positioned at the high temperature shoulder of much larger peaks, which is not possible with any of the classical methods of single peak analysis. In combination with measurements of photocurrent ( $I_{PC}$ ), and its temperature dependence it also enables precise determination of relative trap concentrations and a good estimate of absolute trap concentrations.

## II. MATHEMATICAL ANALYSIS

### A. Single peak analysis

Each deep trap which has been filled with charge carriers at low temperatures will result in a conductivity peak during subsequent heating of the sample due to the release of

trapped charge carriers into the conduction or valence band. For the analysis of TSC spectra some approximations usually have to be made to get analytical solution of the system of rate equations for the emission and retrapping of charge carriers of various traps. One assumption is that concentration of trapped carriers is much greater than the concentration of free carriers, which is easily satisfied for highly resistive or semi-insulating materials. Another assumption is that the lifetime of emitted carriers is dominated by some recombination center<sup>25</sup> which implies that other capture processes (direct recombination, retrapping of charge carriers by the same or by a different trap) may be neglected.

A single peak with no interference (overlaps) of other neighboring peaks obtained with a constant heating rate in TSC scan for above conditions (sometimes called "first-order kinetics"<sup>19</sup>) can be well described as:<sup>26</sup>

$$I_{TSC}(T) = I_0 \exp\left[-\frac{E_a}{kT} - \frac{\nu_0}{\beta} \int_{T_0}^T \exp\left(-\frac{E_a}{kT}\right) dT\right]. \quad (1)$$

The following symbols denote:  $I_0 = N_T e \mu \nu_0 \tau A E[A]$ ; where  $N_T$ : carrier density of the filled traps at the beginning of the temperature ramp ( $\text{cm}^{-3}$ ),  $e$ : the electronic charge  $1.6 \times 10^{-19} [C]$ ,  $\mu$ : the carrier mobility ( $\text{cm}^2/V \text{ s}$ ),  $\nu_0$ : an escape frequency factor ( $\text{s}^{-1}$ ),  $\tau$ : the free carrier lifetime (s),  $A$ : the area of the electrode ( $\text{cm}^2$ ),  $E$ : the applied electric field (V/cm),  $k$ : the Boltzmann's constant  $8.617 \times 10^{-5} (\text{eV/K})$ ,  $\beta$ : the heating rate ( $\text{K s}^{-1}$ ),  $T$ : absolute temperature (K),  $T_0$ : the temperature from which heating begins after complete filling of all deep traps and  $E_a$ : trap activation energy (eV). Instead of the  $I_0$  some authors,<sup>27,28</sup> use  $Q_0/\tau_0$ , where  $Q_0$  denotes total charge released in TSC measurements, while  $\tau_0$  denotes the so-called preexponential factor.

In the same approximation as Eq. (1) free electron concentration,  $n$ , can be evaluated as:<sup>29</sup>

$$n(T) = N_T \tau_n D_t T^2 \exp\left\{-\frac{E_a}{kT} - \frac{kD_t}{\beta E_a} T^4 e^{-E_a/kT}\right. \\ \left. \times \left[1 - 4 \frac{kT}{E_a} + 20 \left(\frac{kT}{E_a}\right)^2\right]\right\}, \quad (2)$$

where  $D_t$  denotes temperature independent coefficient given by

$$D_t = 3.0 \times 10^{21} \left(\frac{m^*}{m_0}\right) \sigma_n \quad (3)$$

with  $m_0$  and  $m^*$  representing electron rest and effective mass, respectively. For GaAs the  $m^*/m_0$  ratio is 0.067.<sup>30</sup>  $\sigma_n$  is practically  $T$  independent for most of deep traps in Si GaAs and similar materials (Ref. 21, p. 108 and Ref. 31, p. 73). However, if  $T$  dependence of  $\sigma_n(T)$  exists, it can be expressed as  $\sigma_n(T) = \sigma_n \exp(-E_{a\sigma}/kT)$ , and in that case  $\sigma_n$  is again  $T$  independent but measured trap activation energy is then equal to  $E_a + E_{a\sigma}$  (Ref. 21, p. 97).

Generally, for predominantly electron conduction the current  $I(T)$  can be expressed as

$$I(T) = K_G \times \mu_n(T) \times n(T), \quad (4)$$

where  $K_G$  denotes geometrical factor,  $K_G = eAE$ . Combining Eqs. (2) and (4) one obtains:

$$I_{\text{TSC}}(T) = N_T e \mu_n A E \tau_n D_i T^2 \times \exp\left[-\frac{E_a}{kT} - \frac{kD_i}{\beta E_a} T^4 e^{-E_a/kT}\right] \times \left[1 - 4 \frac{kT}{E_a} + 20 \left(\frac{kT}{E_a}\right)^2\right]. \quad (5)$$

From Eq. (5) it is evident that amplitude, position, and width of the TSC peak depend on many trap and material properties, i.e., on all main trap parameters ( $E_a$ ,  $\sigma_n$ ,  $N_T$ ), as well as on free electrons lifetime and mobility. In addition it depends on several external parameters, i.e., on heating rate, area of electrodes and applied electric field. Comparing Eqs. (1) and (5) it follows that  $Q_0$  can be expressed as:

$$Q_0 = \frac{I_0}{\nu_0} = I_0 \tau_0 = N_T \tau_n \mu_n K_G. \quad (6)$$

Up to now different fitting procedures were used mainly on single, well resolved, and isolated TSC peaks.<sup>26–29</sup> Equation (5) describes well the TSC curve in rare occasions when one peak is alone and absolutely dominant. However, much more frequently TSC spectra consists of large number of peaks,<sup>10,12–18,32–34</sup> overlapping heavily. This makes single peak analysis often inadequate.

## B. Simultaneous multiple peak analysis (SIMPA)

To avoid difficulties of single peak analysis, in this paper we analyzed all levels simultaneously. For that purpose the fitting function,  $I_{\text{SIMPA}}$ , comprising the sum of all features of the TSC peak spectrum was built as

$$I_{\text{SIMPA}}(T) = \sum_{i=1}^m I_{\text{TSC}}^i(T) + I_{\text{EL2}}, \quad (7)$$

where  $I_{\text{TSC}}^i$  denotes contribution of each peak alone, calculated by means of Eq. (5),  $m$  denotes number of deep traps involved in calculation. In undoped SI GaAs samples conductivity close and above room temperature (RT), is governed by EL2 level.  $I_{\text{EL2}}$  denotes dark current calculated by the following relation:

$$I_{\text{EL2}} = C \exp\left(\frac{-E_{\text{EL2}}}{kT}\right), \quad (8)$$

where  $C$  is a constant, and  $E_{\text{EL2}}$  is the main donor activation energy, expected for EL2 to be  $0.75 \pm 0.02$  eV.<sup>35</sup>

The validity of assumption that the first order kinetics is applicable, can be checked isolating (at least) one single TSC peak, as it was done in Ref. 29. Since this peak can be excellently fitted with Eq. (5), the second order kinetics can be excluded since it would give completely different shape of TSC peaks.<sup>19</sup>

In Eq. (5) there are five unknowns. However, two of them ( $\mu_n$  and  $\tau_n$ ) can be independently determined (see Secs. II C and II D), which reduces the number of fitting parameters to three ( $N_T$ ,  $E_a$ , and  $\sigma_n$ ). Analysis shows, however, that the influence of each of these parameters to peak characteristics can be well resolved:  $N_T$ ,  $E_a$ , and  $\sigma_n$  primarily determine peak height, peak position, and peak width, respectively. Due to the interconnection of these pa-

rameters, the change of  $\sigma_n$  up to 20% from the best fit value can be compensated by the change of  $E_a$  (for  $\sim 1\%$ ) and  $N_T$  (for  $\sim 5\%$ ), still giving fair enough fits. However, for changes of  $\sigma_n$  greater than 20% calculated peak width cannot be compensated any more and becomes considerably different from the measured peak width value. Hence, the uniqueness of the fit is ensured within confidence limits of  $\pm 20\%$ ,  $\pm 1\%$ , and  $\pm 5\%$ , for  $\sigma_n$ ,  $E_a$ , and  $N_T$ , respectively.

From the best fit of the whole TSC spectra, the trap's signature, namely  $E_a$ 's and  $\sigma_n$ 's can be simultaneously extracted for all traps present in the material, as well as their  $T_m$ 's. Furthermore, another benefit of the SIMPA method is the possibility to calculate more precisely, the effectively collected charge,  $Q_{T_i}$ , released from the  $i$ th trap, since each trap is now well resolved and separated from the rest of the spectra. This can be done by the following relation:

$$Q_{T_i} = \int I_{\text{TSC}}^i dt = \frac{1}{\beta} \int_{T_0}^T I_{\text{TSC}}^i dT, \quad (9)$$

where  $dt = 1/\beta dT$ .  $Q_{T_i}$  collected at the contacts is only a fraction of the total charge emitted from  $i$ th trap,  $Q_{T_i}^{\text{tot}}$ . To calculate  $Q_{T_i}^{\text{tot}}$ , which is proportional to the  $i$ th trap concentration,  $N_{T_i}$ , corrections due to the  $T$  dependence of free electron lifetime,  $\tau_n(T)$  (and consequently fraction of actually collected charge in comparison with real charge emitted from each trap), as well as corrections due to the mobility [ $\mu_n(T)$ ] temperature dependence have to be made. Knowing  $\tau_n$  and  $\mu_n$  at one temperature, for example at liquid nitrogen temperature (LNT),  $\tau_n(\text{LNT})$ , and  $\mu_n(\text{LNT})$ , measured the charge emitted from  $i$ th trap, having a maximum at  $T_i$ , can be renormalized to the same measurement sensitivity via

$$Q_{T_i}^{\text{tot}} = F_Q \times Q_{T_i}, \quad (10)$$

where  $F_Q$  is a charge correction factor defined as

$$F_Q = \frac{\tau_n(\text{LNT}) \times \mu_n(\text{LNT})}{\tau_n(T_i) \times \mu_n(T_i)}. \quad (11)$$

## C. Determination of relative trap concentrations

Due to longer  $\tau_n$  and larger  $\mu_n$  values at low temperatures the sensitivity of TSC increases with the lowering of  $T$ , so that resulting in TSC peaks at low  $T$  appear relatively higher than high  $T$  peaks. In the measured temperature range (85–300 K),  $\mu_n(T)$  for undoped GaAs can be well approximated with  $T^{-2.2}$  function. The use of actually measured values for  $\mu_n$ <sup>36</sup> instead of the  $T^{-2.2}$  dependence would give a correction of only 2%–3%. For determination of relative trap concentrations, renormalized charge values ( $Q_{T_i}^{\text{tot}}$ ) should be taken. Taking into account both  $\tau_n(T)$  and  $\mu_n(T)$  corrections, for two deep traps  $i$  and  $j$ , relative concentrations can be calculated from

$$\frac{N_i}{N_j} = \frac{Q_{T_i} \times \tau_{n,T_j}}{Q_{T_j} \times \tau_{n,T_i}} \times \left(\frac{T_j}{T_i}\right)^{-2.2}. \quad (12)$$

The expression demonstrates how incorrect it would be to determine relative trap concentrations just from the inten-

sities of respective TSC peaks in the same sample at different  $T$ , as well as among different samples if  $\tau_n$  is not determined independently.

### D. Estimate of absolute trap concentrations

Generally, the photocurrent is proportional to the free electron lifetime. For SI-GaAs, in the LNT to RT range,  $I_{PC}(T)$  reflects  $\tau_n(T)$  behavior.<sup>37</sup> This temperature dependence is expected to be exponential.<sup>13,25</sup> Measurements of  $I_{PC}(T)$  on the same set of samples,<sup>38</sup> actually confirmed an approximately exponential decrease of  $I_{PC}$  with temperature, resulting in approximately three orders of magnitude lower  $\tau_n$  at RT in comparison with the LNT value. Knowing the  $\tau_n(T)$  dependence enables the sensitivity correction of TSC signal at each  $T$  to be made.

For quantitative evaluations of trap concentrations the  $\tau_n(T)$  values need to be known. We calculated  $\tau_n$  at LNT temperature,  $\tau_n(\text{LNT})$  following the analysis of Look,<sup>21</sup> for SI-GaAs. The concentration of photogenerated electrons is connected with  $\tau_n$  via

$$n = F \tau_n, \quad (13)$$

where  $F$  denotes free electrons generation rate, defined as:  $F = \Phi \alpha$ .  $\Phi$  denotes effective monochrome light flux (in photons/cm<sup>2</sup> s), for our experimental conditions defined as  $\Phi = \Phi_0(1 - e^{-\alpha d})/\alpha d$ :  $\alpha$  is absorption coefficient;  $\Phi$  can be evaluated measuring  $\alpha$ , and knowing sample thickness  $d$ .<sup>39</sup>

On the other hand,  $n$  is also related with saturation photocurrent,  $I_{PC}^\infty$ , in analogy with Eq. (4):

$$I_{PC}^\infty = K_G \times \mu_n \times n. \quad (14)$$

Combining Eqs. (13) and (14)  $\tau_n(\text{LNT})$  can be calculated.

Trap concentration,  $N_{T_i}$ , can now be estimated from the standard relation:<sup>34</sup>

$$N_{T_i} = \frac{Q_{T_i}}{V_{\text{eff}} \times e \times G}, \quad (15)$$

where  $Q_{T_i}$  denotes temporal integral of  $I_{TSC}^i$ ,  $V_{\text{eff}}$  denotes effective illuminated volume of the sample, and  $G$  the collection factor. Assuming a uniform distribution of the electric field through the specimen, collection factor is generally defined as  $G = \mu_n \tau_n V / L^2$ , where  $L$  and  $V$  denote distance between electrodes and bias applied to the specimen, respectively.

On the other hand, following Eq. (6) the absolute trap concentration,  $N_{T_i}$ , can also be expressed as:

$$N_{T_i} = \frac{Q_{T_i}}{2 \times \tau_n(T_i) \times \mu_n(T_i) \times K_G}. \quad (16)$$

The factor 1/2 is added for the correction of the induced current assuming uniform distribution of  $N_{T_i}$ .<sup>34</sup>

Both Eqs. (15) and (16), can then be used to calculate absolute trap concentrations.

## III. RESULTS AND DISCUSSION

Figure 1 presents an example of typical experimental TSC spectra obtained from an ‘‘old’’ sample (produced in

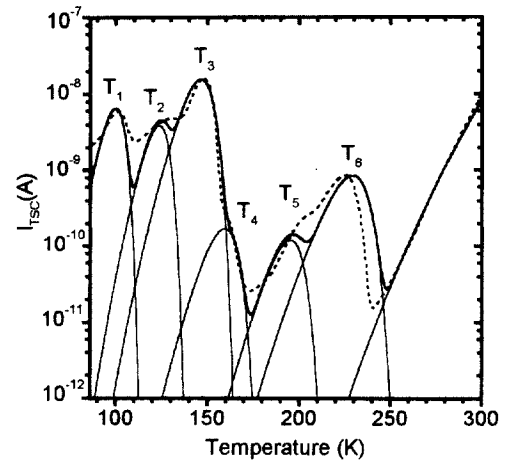


FIG. 1. Experimental TSC curve and its fit based on single peak analysis data. The thick dotted line denotes typical TSC spectra (measured on ‘‘old’’ sample with large deep trap concentrations), obtained after all deep traps have been filled by adequate illumination at 86 K. Thin solid lines denote particular TSC peaks (components) calculated by means of Eq. (5) and using parameters, for each trap obtained from single peak analysis (Refs. 16 and 17). Dark band current was calculated from Eq. (8). Thick solid curve presents the sum of single peaks as in Eq. (7).

the late 1980s) and its fit based on a single peak analysis. These samples have been used here since they have relatively large deep trap concentrations and because a wealth of experimental data have been reported on this type of samples (having the same or similar TSC spectra). The thick dotted line denotes measured TSC spectra; peaks are denoted as  $T_1, \dots, T_6$ , in accordance with the previous notation.<sup>1,16,32,40</sup> The same levels are present in TSC results of many research groups.<sup>1,2,12–17,34,40</sup> To fit this spectrum with results obtained from the single peak analysis, the trap parameters for each of these peaks were taken as follows: Set of  $\sigma_n$ 's, for each peak determined from partial trap filling,<sup>18</sup> and trap filling/emptying dynamics,<sup>41</sup> with the only difference that the more correct LNT value of  $\mu_n = 10^5 \text{ cm}^2/\text{V s}$ <sup>39</sup> was used here.  $T_m$  values were deduced from experimental TSC curve and  $E_a$  values were calculated from the usual approximations.<sup>16,17</sup> All deep trap parameter values are presented in Table I. The slope of the straight line around RT was 0.73 eV, which corresponds well with expected EL2 value.<sup>35</sup>

Thin solid lines denote particular TSC peaks (components) each calculated by means of Eq. (5), and the dark current calculated from Eq. (8). A thick solid line is obtained by summing up data resulting from a single peak analysis,

TABLE I. Deep trap parameters for TSC peaks presented in Fig. 1, obtained from single peak analysis.<sup>a</sup>

Level	$T_m$ /K	$E_a$ /eV	$\sigma_n/\text{cm}^2$
$T_1$	98	0.160	$7.0 \times 10^{-18}$
$T_2$	127	0.230	$8.0 \times 10^{-17}$
$T_3$	145	0.257	$1.0 \times 10^{-17}$
$T_4$	157	0.283	$1.0 \times 10^{-17b}$
$T_5$	198	0.431	$1.0 \times 10^{-15}$
$T_6$	225	0.485	$2.0 \times 10^{-16}$

<sup>a</sup>See Refs. 16–18 and 41.

<sup>b</sup>Estimated value.

for peaks  $T_1 - T_3$  and  $T_5$  and  $T_6$  plus the addition of peak  $T_4$  with estimated  $\sigma_n$ . Trap concentrations were taken to allow the best possible accordance between calculated and experimental TSC spectra.

As one can see from Fig. 1, single peak analysis parameters do not give a satisfactory accordance of experimental and calculated curves, for some of the deep traps and particularly for the whole TSC spectrum. This is so because in characterizing a particular single peak, interference from neighboring peaks cannot be completely excluded nor evaluated and errors in obtained parameters seem to be unavoidable. These discrepancies become especially evident when the fit of the whole TSC spectrum is compared with actual experimental spectrum, since then the errors from each single peak are summing up. It also becomes clear why and how simultaneous fitting of all peaks can improve fitting of the whole TSC spectra:

(1) For all TSC peaks SIMPA enables simultaneous optimization of  $\sigma_n$ 's and  $E_a$ 's, as well as all other trap parameters, minimizing total error, and through that minimizing errors in parameters of each peak.

(2) It can be seen from the Fig. 1, where TSC peaks are "missing," i.e., whether some additional trap(s) have to be included into analysis. In this particular TSC the curve traps  $T_0$  with a maximum at approximately 85 K and  $T_{4a}$  (177 K) as well as  $T_7$  (250 K) must be added.

(3) It is clear that some peaks, like  $T_2$ , for example, should be much broader to improve in accordance with the experiment. When that was attempted, unphysically small  $\sigma_n$  has been obtained. Hence, it becomes clear that  $T_2$  has to be a composite peak consisting of two closely positioned peaks, and needs to be split in two close peaks  $T_{2a}$  and  $T_{2b}$  with similar activation energies and concentrations.

(4) For small TSC peaks ( $T_4$ , for example), being positioned at the high  $T$  shoulder of regularly much larger peak ( $T_3$ ), it is practically impossible to determine  $\sigma_n$  by any of the classical methods of TSC analysis, based on a single peak analysis. Now, using SIMPA method this becomes possible.

Fitting results (for the same experimental TSC spectrum) obtained after the above remarks were included via SIMPA analysis, are presented in Fig. 2(a). Very good accordance of  $I_{\text{SIMPA}}$  (thick solid curve) and experimental TSC (thick dotted curve) is achieved, for the whole TSC spectra. Particular TSC peak contributions are again presented as thin solid curves. Complete sets of main parameters, taken from the best-fit curve, obtained simultaneously for all traps, are given in the Table II(a). In this paper, we obtained clearly separated contributions of each particular deep level, with each trap having its own unique and distinguished "signature."

SIMPA analysis implies that  $T_2$  consists of two closely spaced levels  $T_{2a}$  and  $T_{2b}$ , with maxima at 114 and 127 K, and  $E_a$  values of 0.204 and 0.233 eV, respectively. Insets of Figs. 2(a) and 2(b) emphasize the need of more than one peak between  $T_1$  and  $T_3$  in 105–135 K temperature range. The choice of particular parameters for the  $T_{2a}$  and  $T_{2b}$  peak becomes clearer in samples where the concentration of either  $T_{2a}$  or  $T_{2b}$  is considerably larger than the other as shown in Ref. 42. In samples where concentrations of these neighbor-

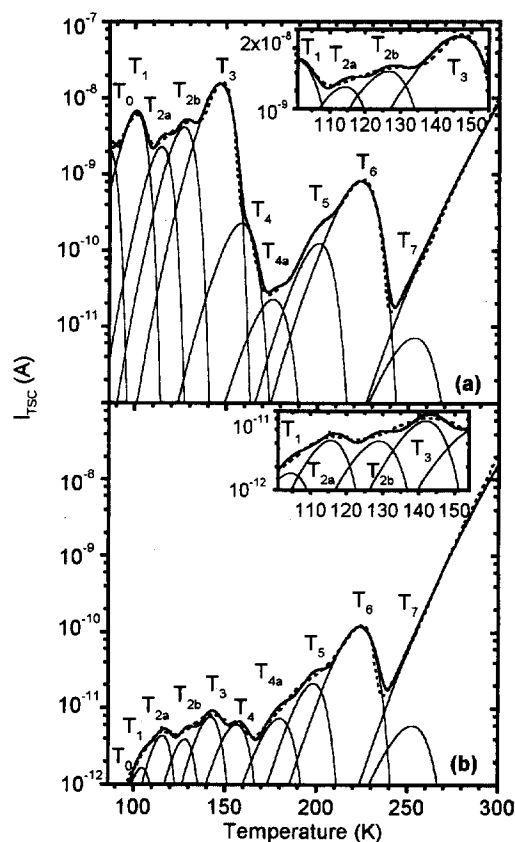


FIG. 2. (a) Experimental and calculated TSC curves for the same sample as in Fig. 1 and for "new" sample 2b using simultaneous fitting of the whole TSC spectrum. The thick dotted line denotes measured TSC spectra after all deep traps have been filled by adequate illumination at 86 K. Thin solid lines denote particular TSC peaks (components) calculated by means of Eq. (5), and the dark band current calculated from Eq. (8). The thick solid curve presents the best fit,  $I_{\text{SIMPA}}$  obtained by Eq. (7). Insets of (a) and (b) show the same but in narrower  $T$  ranges.

ing peaks would differ significantly, two closely positioned but clearly distinguishable peaks should be noticed in TSC spectra. Levels very close to SIMPA predictions were indeed observed by Fang *et al.*;<sup>17</sup>  $T_m = 114$  K, 125 K, and  $E_a = 0.21$  eV, 0.23 eV, respectively. These levels also correspond to 111 K (0.19 eV) and 126 K (0.22 eV)  $b$  and  $c$  levels reported by Lin *et al.*<sup>14</sup> These two traps have also very similar  $\sigma_n$  values ( $3 \times 10^{-17}$  cm<sup>-2</sup>,  $4 \times 10^{-17}$  cm<sup>-2</sup>), and this is probably the reason why many other authors, probably also having samples similar to ours, with comparable concentrations of these levels declared it as a single level.

SIMPA implies that there is a peak  $T_0$ , situated at the very edge of our TSC spectra, for the applied temperature range. Its  $T_m$  is estimated to be at 85 K, with  $E_a = 0.145$  eV and  $\sigma_n = 3.3 \times 10^{-17}$  cm<sup>-2</sup> with concentration of  $1.9 \times 10^{13}$  cm<sup>-3</sup>. This level corresponds with peak  $d$  in the paper of Tomozane and Nannichi,<sup>34</sup> with maximum situated at 83 K, attributed to electron trap, with concentration around  $2.6 \times 10^{13}$  cm<sup>-3</sup> in their samples.

The existence of the  $T_4$  level was often reported in the literature,<sup>13,17,18,32,35</sup> but it has not been fully characterized because it usually has small concentrations relative to the nearby  $T_3$  peak. Being positioned at the high  $T$  shoulder of a regularly much larger peak  $T_3$ , it is practically inaccessible

TABLE II. Deep trap parameters from the best fit of typical sample TSC spectra.

(a) "Old" sample [presented in Fig. 2(a)]							
Level	$T_m$ /K	$E_a$ /eV	$\sigma_n$ /cm <sup>2</sup>	$Q_T$ /nC	$F_Q$	$N_T^a$ /cm <sup>-3</sup>	$N_T^b$ /cm <sup>-3</sup>
$T_0$	85	0.145	$3.3 \times 10^{-17}$	55.1	1	$1.9 \times 10^{13}$	$1.7 \times 10^{13}$
$T_1$	100	0.158	$2.0 \times 10^{-18}$	196.2	5	$2.5 \times 10^{14}$	$2.3 \times 10^{14}$
$T_{2a}$	114	0.204	$3.0 \times 10^{-17}$	68.2	21	$3.1 \times 10^{14}$	$2.8 \times 10^{14}$
$T_{2b}$	127	0.233	$4.0 \times 10^{-17}$	129.4	38	$1.9 \times 10^{15}$	$1.7 \times 10^{15}$
$T_3$	146	0.277	$5.1 \times 10^{-17}$	641.8	129	$2.0 \times 10^{16}$	$1.8 \times 10^{16}$
$T_4$	156	0.284	$1.3 \times 10^{-17}$	9.9	377	$8.9 \times 10^{14}$	$8.1 \times 10^{14}$
$T_{4a}$	177	0.315	$0.9 \times 10^{-17}$	1.0	722	$1.7 \times 10^{14}$	$1.5 \times 10^{14}$
$T_5$	200	0.443	$0.9 \times 10^{-15}$	5.6	2039	$2.7 \times 10^{15}$	$2.5 \times 10^{15}$
$T_6$	225	0.488	$4.5 \times 10^{-16}$	45.6	4409	$4.8 \times 10^{16}$	$4.4 \times 10^{16}$
$T_7$	253	0.522	$0.8 \times 10^{-16}$	0.4	7783	$8.3 \times 10^{14}$	$7.5 \times 10^{14}$
$\Sigma N_T^{\text{"old"}} = 8.8 \times 10^{16}$							
(b) "New" sample [presented in Fig. 2(b)]							
Level	$T_m$ /K	$E_a$ /eV	$\sigma_n$ /cm <sup>2</sup>	$Q_T$ /pC	$N_T^a$ /cm <sup>-3</sup>	$N_T^b$ /cm <sup>-3</sup>	$\frac{N_T^{\text{"old"}}}{N_T^{\text{"new"}}$
$T_0$	83	0.150	$3.3 \times 10^{-17}$	5.4	$2.2 \times 10^9$	$2.2 \times 10^9$	8756
$T_1$	103	0.163	$2.3 \times 10^{-18}$	52.6	$1.1 \times 10^{11}$	$1.1 \times 10^{11}$	2261
$T_{2a}$	115	0.207	$2.8 \times 10^{-17}$	149.6	$1.2 \times 10^{12}$	$1.3 \times 10^{12}$	250
$T_{2b}$	127	0.235	$4.0 \times 10^{-17}$	134.9	$2.0 \times 10^{12}$	$2.0 \times 10^{12}$	920
$T_3$	144	0.268	$5.2 \times 10^{-17}$	297.9	$1.5 \times 10^{13}$	$1.6 \times 10^{13}$	1307
$T_4$	153	0.277	$1.0 \times 10^{-17}$	251.1	$3.7 \times 10^{13}$	$3.8 \times 10^{13}$	24
$T_{4a}$	178	0.324	$1.0 \times 10^{-17}$	309.9	$8.8 \times 10^{13}$	$8.9 \times 10^{13}$	2
$T_5$	198	0.437	$0.9 \times 10^{-15}$	814.8	$6.6 \times 10^{14}$	$6.7 \times 10^{14}$	4
$T_6$	225	0.497	$7.4 \times 10^{-16}$	6352	$1.1 \times 10^{16}$	$1.1 \times 10^{16}$	4
$T_7$	253	0.520	$0.8 \times 10^{-16}$	450	$6.8 \times 10^{14}$	$6.2 \times 10^{14}$	1.2
$\Sigma N_T^{\text{"new"}} = 1.2 \times 10^{16}$							
						7.3	

<sup>a</sup>Calculated by Eq. (15).  
<sup>b</sup>Calculated by Eq. (16).

by any method of single peak TSC analysis (initial rise–initial fall, etc.) SIMPA gives  $\sigma_n$  to be  $1.3 \times 10^{-17}$  cm<sup>2</sup>, with concentration close to  $10^{15}$  cm<sup>-3</sup> range.

Introduction of the  $T_{4a}$  level although with a very small concentration greatly improved initial fitting, because it filled the gap between  $T_4$  and  $T_5$  levels. This level, with  $T_m$  at 177 K, and  $E_a = 0.315$  eV frequently went unnoticed. Some authors<sup>43,44</sup> reported levels near that position but without detailed characterization, due to small concentration.

The strength of SIMPA method is nicely demonstrated in the case of peak  $T_7$ . Although there is not even the slightest hint of a peak in our TSC spectrum, SIMPA fitting showed that there exists a deep trap, with maximum around 250 K,  $E_a = 0.522$  eV and  $\sigma_n = 0.8 \times 10^{-16}$  cm<sup>2</sup>. However, a deep level at exactly that position was reported by many research groups.<sup>13,14,17,32</sup> Sometimes it is represented with a prominent and even dominant peak in TSC spectrum.<sup>32</sup>

Similar trap concentrations are obtained calculated either from Eq. (15) or Eq. (16). Values obtained for peaks  $T_2, T_5, T_6$  are comparable with those reported by Fang *et al.*,<sup>17</sup> while in the case of  $T_0, T_5,$  and  $T_6$  with those reported by Tomozane and Nannichi<sup>34</sup> in their samples.

Generally, trap concentrations obtained for "old" samples [reported in Fig. 2(a)] range between  $2 \times 10^{13}$  and  $5 \times 10^{16}$  cm<sup>-3</sup>. Simulated  $E_{EL2}$  depth was 0.73 eV, which is in accordance with expectations for EL2 level.<sup>35</sup>

Figure 2(b) presents fitting results (thick solid curve) of measured typical TSC spectra (thick dotted line) from other types of samples, having much lower deep trap concentrations ("new" samples produced in mid 1990s). One can conclude that  $I_{SIMPA}$  is again in very good agreement with experiment. The important result is that the best fit curve is obtained with exactly the same traps (the same "trap signatures" within experimental errors) as for "old" samples. The only difference is a much smaller concentration of some of those traps. Results are given in Table II(b).

Ten different levels are again present in this fit, but most of them with considerably reduced concentrations, compared to "old" samples. Concentration ratios are given in the last column of Table II(b). Reduction of trap concentrations differ considerably for two different trap groups. For low-temperature peaks ( $T_0 - T_3$ ) reduction goes for almost four orders of magnitude, while for peaks situated above 150 K the reduction is only one order of magnitude or less. This may be an important fact in trap identification, because, in "new" samples only  $T_5$  and  $T_6$  retain relatively high trap concentrations (around  $10^{16}$  cm<sup>-3</sup>). Furthermore, the  $T_7$  trap is the only one whose concentration remains the same in both types of samples. It is also important that the reduction of the total deep level concentration (for  $\sim$  factor 7) is less than it would appear from the first glance at TSC spectra,

since the least reduced traps were those having the highest concentrations.

The well-defined SIMPA procedure presented for the quantitative analysis of TSC spectra enabled a systematic study of a very large number of SI-GaAs samples produced in a period of over a decade by more than ten different manufacturers. Measured TSC spectra of various samples and calculated deep trap concentrations vary many orders of magnitude. However, it is interesting and important that a number of different deep levels needed to obtain excellent fits in all these samples<sup>42</sup> was limited to only eleven specific levels, the difference being only in their relative and absolute concentrations.

#### IV. CONCLUSIONS

In this paper we presented a new analytical method which enables simultaneous fitting of the whole measured TSC spectra. Simultaneous multiple peak analysis (SIMPA) method overcomes most problems of a single peak analysis methods and enables simultaneous determination of main peak parameters of all traps present in the material (trap signatures). In combination with measurements of photocurrent ( $I_{PC}$ ) and its temperature dependence, which reflects  $\tau_n$  temperature dependence, it also enables precise determination of relative trap concentrations and a good estimate of absolute trap concentrations.

SIMPA method considerably improves the analysis of TSC spectra in comparison with single peak approach. Following facts greatly improved reliability of the results.

(1) In any single peak analysis parameters of each peak are determined independently of other peaks, so that errors are just summing up resulting in a quite erroneous fit of the whole TSC spectra (Fig. 1). In SIMPA, fitting of the whole TSC spectra enables simultaneous optimization of  $\sigma_n$ 's, as well as all other trap parameters, so that the sum of errors for all deep traps is minimized.

(2) SIMPA clearly indicates where TSC peaks are "missing," showing that some additional traps with calculable concentrations have to be included into analysis.

(3) SIMPA shows (predicts) when some peak is composite, and needs to be split in two close peaks.

(4) For small TSC peaks, including those being positioned at the high  $T$  shoulder of much larger peaks, SIMPA can determine all traps parameters, including determination of  $\sigma_n$ . This is not possible by any of classical methods of TSC analysis (Arrhenius plots, initial rise–initial fall method, standard approximate formulas,<sup>16,17</sup> etc.).

For all these reasons the SIMPA method gives a more complete and more reliable set of parameters for each deep trap present in the TSC spectra.

Another important result of this study is that the best fits are obtained with the same set of trap parameters (up to 11 different traps), for SI-GaAs samples having dramatically different TSC spectra. The only difference was relative and absolute concentration of these different traps.

We conclude that SIMPA method is very promising for the characterization of deep levels in some other SI materials, like SI-InP and SI-CdTe.

- <sup>1</sup>U. V. Desnica and B. Šantić, Appl. Phys. Lett. **54**, 810 (1989).
- <sup>2</sup>W. C. Mitchel and J. Jimenez, J. Appl. Phys. **75**, 3060 (1994).
- <sup>3</sup>U. V. Desnica, D. I. Desnica, and B. Šantić, Appl. Phys. Lett. **58**, 278 (1991).
- <sup>4</sup>J. Jimenez, M. A. Gonzales, P. Hernandez, and J. A. de Saja, J. Appl. Phys. **57**, 1152 (1985).
- <sup>5</sup>J. Jimenez, P. Hernandez, and J. A. de Saja, Solid State Commun. **55**, 459 (1985).
- <sup>6</sup>H. J. Queisser, Ann. Phys. (Leipzig) **47**, 461 (1990).
- <sup>7</sup>U. V. Desnica, D. I. Desnica, and B. Šantić, J. Phys.: Condens. Matter **3**, 5817 (1991).
- <sup>8</sup>T. Benchigner, B. Mari, C. Schwab, and U. V. Desnica, Jpn. J. Appl. Phys. **31**, 2669 (1992).
- <sup>9</sup>M. Beaumler, U. Kaufmann, and J. Windscheif, Appl. Phys. Lett. **46**, 781 (1985).
- <sup>10</sup>U. V. Desnica and B. Šantić, J. Appl. Phys. **67**, 1408 (1990).
- <sup>11</sup>J. Jimenez, P. Hernandez, J. A. de Saja, and J. Bonafé, Phys. Rev. B **35**, 3832 (1987).
- <sup>12</sup>Z.-Q. Fang and D. Look, Mater. Sci. Forum **83–87**, 991 (1992).
- <sup>13</sup>A. A. Lin and R. H. Bube, J. Appl. Phys. **47**, 1859 (1976).
- <sup>14</sup>A. L. Lin, E. Omelianovski, and R. H. Bube, J. Appl. Phys. **47**, 1852 (1976).
- <sup>15</sup>B. Šantić and U. V. Desnica, Appl. Phys. Lett. **56**, 2636 (1990).
- <sup>16</sup>D. I. Desnica, J. Electron. Mater. **21**, 463 (1992).
- <sup>17</sup>Z.-Q. Fang, L. Shan, T. E. Schlesinger, and A. G. Milnes, Mater. Sci. Eng., B **5**, 397 (1990).
- <sup>18</sup>B. Šantić, U. V. Desnica, N. Radić, D. Desnica, and M. Pavlović, *Proceedings of 7th Conference on Semi-Insulating Materials, Ixtapa, Mexico, 1992*, edited by C. Miner (IOP, Bristol, 1993), Chap. 7, p. 241.
- <sup>19</sup>R. Fasbender, G. Hirt, M. Thoms, and A. Winacker, Semicond. Sci. Technol. **11**, 935 (1996).
- <sup>20</sup>G. M. Martin and D. Bois, Proc. Electrochem. Soc. **78**, 32 (1978).
- <sup>21</sup>D. C. Look, *Semiconductors and Semimetals* (Academic, New York, 1983), Vol. 19.
- <sup>22</sup>R. E. Kremer, M. C. Arikian, J. C. Abele, and J. S. Blakemore, J. Appl. Phys. **62**, 2424 (1987).
- <sup>23</sup>J. C. Abele, R. E. Kremer, and J. S. Blakemore, J. Appl. Phys. **62**, 2432 (1987).
- <sup>24</sup>P. K. Giri and Y. N. Mohapatra, J. Appl. Phys. **78**, 262 (1995).
- <sup>25</sup>J. S. Blakemore, *Semiconductor Statistics* (Pergamon, New York, 1962), p. 280.
- <sup>26</sup>S. Maeta and F. Yoshida, Jpn. J. Appl. Phys. **28**, 1712 (1989).
- <sup>27</sup>J. Prakash, R. Nishad, and A. K. Nishad, J. Appl. Phys. **59**, 2129 (1986).
- <sup>28</sup>C. Christodoulides, L. Apekis, and P. Pissis, J. Appl. Phys. **64**, 1367 (1988).
- <sup>29</sup>B. Šantić, N. Radić, and U. V. Desnica, Solid State Commun. **79**, 535 (1991).
- <sup>30</sup>J. S. Blakemore, J. Appl. Phys. **53**, R123 (1982).
- <sup>31</sup>R. H. Bube, *Photoconductivity of Solids* (Wiley, New York, 1967), p. 73.
- <sup>32</sup>M. Pavlović, B. Šantić, and U. V. Desnica, J. Phys. D **28**, 934 (1995).
- <sup>33</sup>Z. Q. Fang and D. C. Look, J. Appl. Phys. **69**, 8177 (1991).
- <sup>34</sup>M. Tomozane and Y. Nannichi, J. Appl. Phys. **25**, L273 (1986).
- <sup>35</sup>Z.-Q. Fang and D. C. Look, J. Electron. Mater. **22**, 1361 (1993).
- <sup>36</sup>D. C. Look, *Electrical Characterization of GaAs Materials and Devices* (Wiley, New York, 1989), p. 95.
- <sup>37</sup>R. H. Bube, J. Appl. Phys. **31**, 315 (1959).
- <sup>38</sup>U. V. Desnica, D. I. Desnica, and B. Šantić, Appl. Phys. A **51**, 379 (1990).
- <sup>39</sup>G. M. Martin and S. Makram-Ebeid, in *Deep Centers in Semiconductors*, edited by S. T. Pantelides (Gordon and Breach, New York, 1986), Chap. 6, p. 399.
- <sup>40</sup>H. Yoshida, M. Kiyama, T. Takebe, K. Fujita, and S. Akai, Jpn. J. Appl. Phys. **36**, 19 (1997).
- <sup>41</sup>U. V. Desnica, M. Pavlović, D. I. Desnica, B. Šantić, and T. Šmuc, Mater. Sci. Forum **143–147**, 353 (1994).
- <sup>42</sup>M. Pavlović and U. V. Desnica (unpublished).
- <sup>43</sup>J. C. Abele, R. E. Kremer, and J. S. Blakemore, J. Appl. Phys. **62**, 2432 (1987).
- <sup>44</sup>A. Mircea and A. Mittonneau, Appl. Phys. **8**, 15 (1975).